

## Response to reviewers for the paper “HO<sub>x</sub> and NO<sub>x</sub> production in oxidation flow reactors via photolysis of isopropyl nitrite, isopropyl nitrite-d<sub>7</sub>, and 1,3-propyl dinitrite at λ = 254, 350, and 369 nm.”

We thank the reviewers for their comments on our paper. To guide the review process we have copied the reviewer comments in black text. Our responses are in regular blue font. We have responded to all the referee comments and made alterations to our paper (in bold text).

### Anonymous Referee #2

Summary and overall review: This manuscript evaluates the use of alkyl nitrite (AN) photolysis as an OH-precursor in an oxidation flow reactor (OFR). Experimental and model simulation approaches are used to constrain the parameters of interest to OFR studies such as the actinic flux calibration, amount of OH and NO<sub>x</sub> generation for different types of ANs as precursors. Empirical calibration equations are fit to observed data to create a domain of different OFR operational parameters such as residence time, external reactivity, etc. within which future AN-OFR experiments may operate. Finally, using chemical ionization mass spectrometry, it is shown that molecular structures of α-pinene SOA formed in the AN-OFR bear resemblance to that of ambient SOA previously observed in terpene-rich environments. The manuscript is topically relevant to AMT and builds on the body of literature regarding OFRs. However there are several shortcomings in the experimental description, outlined in my comments below, that must be addressed before it is ready for publication.

R2.1): The manuscript would benefit from a clearer description of the conditions when a PAM/OFR user would want to deploy nitrite as the OH precursor instead of using OFR185, OFR254, or injecting HONO. This manuscript demonstrates that AN can be used as a HO<sub>x</sub> precursor, but putting this method into better context with existing OFR practices would improve the manuscript.

Please see our response and updates to the paper text in response to a similar comment R.1.1 regarding comparison of OFR369-i(iPrONO) and OFR185/OFR254-iN<sub>2</sub>O. We anticipate that HONO will not be a useful HO<sub>x</sub> precursor in OFRs, as discussed in a new subsection below (please note that section has changed from Section 3.3.x to Section 3.5.x in response to comment 2.18):

#### 3.5.2 Nitrous acid (HONO)

HONO is also commonly used as an OH radical source in environmental chamber studies. To evaluate its potential application in OFRs, we examined previous measurements in an environmental chamber equipped with blacklights, where photolysis of 3-20 ppm HONO generated initial [OH]~6×10<sup>7</sup> molecules cm<sup>-3</sup> (Cox et al., 1980) which is 3.3 times lower than [OH] obtained from comparable levels of MeONO (Section 3.5.1). Lower OH<sub>exp</sub> achieved from HONO photolysis is presumably due to higher OH reactivity of HONO relative to MeONO/iPrONO. Additionally, HONO is difficult to prepare without NO<sub>2</sub> impurities (Febo et al., 1995) that may cause additional OH suppression. For these reasons, we believe that

there is no advantage to using HONO as a HO<sub>x</sub> precursor in OFRs.

We have added the following references:

**A. Febo, C. Perrino, M. Gherardi, and R. Sparapani. Evaluation of a High-Purity and High-Stability Continuous Generation System for Nitrous Acid. Environmental Science & Technology 1995 29 (9), 2390-2395. DOI: 10.1021/es00009a035.**

**Richard A. Cox, Richard G. Derwent, and Michael R. Williams. Atmospheric photooxidation reactions. Rates, reactivity, and mechanism for reaction of organic compounds with hydroxyl radicals Environmental Science & Technology 1980 14 (1), 57-61. DOI: 10.1021/es60161a007**

R2.2) OH estimation from SO<sub>2</sub> and sulfate: (i) What collection efficiency was assumed for sulfate particles in the ACSM? (ii) An example of the sulfur mass balance should be shown (e.g., SO<sub>2</sub> inlet, SO<sub>2</sub> that survives the OFR, particulate SO<sub>4</sub>, SO<sub>2</sub> lost to walls or other surfaces), at least in the SI.

(i) We assumed CE = 1, but for our purpose, the absolute CE value doesn't matter provided that the CE of sulfuric acid particles generated by SO<sub>2</sub> + OH via conventional OFR254 or via alkyl nitrite photolysis is the same. This assumption is justified based on the fact the humidity was similar for OFR254 and alkyl nitrite experiments and no ammonia (aside from presumably trace background levels) were present.

We modified the text as follows:

P4-5,L31-2: “ To relate the measured [SO<sub>2,0</sub>] and sulfate to OH<sub>exp</sub>, we conducted an offline calibration where 493 ppb SO<sub>2</sub> was added to the reactor and OH was generated via O<sub>3</sub> + hv254 → O(<sup>1</sup>D) + O<sub>2</sub> followed by O(<sup>1</sup>D) + H<sub>2</sub>O → 2OH in the absence of NO<sub>x</sub>. The reactor was operated at the same residence time **and humidity** used in alkyl nitrite experiments, **although we note that humidity will not change the response of the ACSM to sulfuric acid aerosols. Because no particulate ammonia was present aside from trace background levels, we assumed an ACSM collection efficiency of unity for the sulfate particles.**”

(ii) A sulfur mass balance is not possible because we could not unambiguously measure the SO<sub>2</sub> that survives the OFR due to apparent interferences in the SO<sub>2</sub> measurement (P4, L28). We added a new supplemental figure that illustrates this:

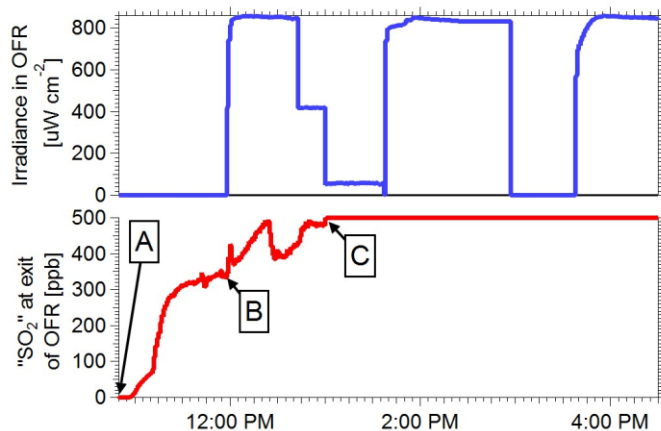


**Figure S5.** Example time series of SO<sub>2</sub> mixing ratio and irradiance (UV intensity) measured during a representative OFR369-i(iPrONO) OH<sub>exp</sub> calibration. (A) Began SO<sub>2</sub> addition at OFR inlet with lamps off; 9.3 ppm iPrONO also added

R2.3) OH<sub>exp</sub> estimation in Section 2.2.2: This work achieves < 1 day of OH<sub>exp</sub> and thus the uncertainties with estimating OH<sub>exp</sub> warrant more attention. One of the earlier OFR studies by Lambe et al. (2011) accounted for the influence of humidity on the growth of H<sub>2</sub>SO<sub>4</sub> particles upon SO<sub>2</sub> oxidation in the OFR. This section describes how calibration of OH<sub>exp</sub> v. particulate sulfate (from conventional OFR-254 method, hence in presence of humidity) was applied to measured particulate sulfate (from iPrONO photolysis, presumably also with humidity) to estimate OH<sub>exp</sub>.

R2.3a): It would be beneficial to briefly discuss how humidity was controlled in both these experiments and whether or not it was accounted for in correction of ACSM measured sulfate mass (unless sample was dried prior to ACSM sampling, in which case that should be specified).

We modified the text as follows:

P3, L11: "The relative humidity (RH) in the reactor was controlled in the range of 31-63% at 21-32°C using a Nafion humidifier (Perma Pure LLC), with corresponding H<sub>2</sub>O volumetric mixing ratios of approximately 1.5-1.7%.

Please also see our response to R2.2, where we note that humidity does not affect the ACSM response to sulfuric acid aerosols.

R2.3b): It is not surprising that the sulfate mass responded linearly to increasing [SO<sub>2,0</sub>] in both these systems. The purpose of doing this inter-comparison was to see how much mass is formed

in the iPrONO system v. in the conventional OFR-254 system, which would then imply how much OH<sub>exp</sub> is achieved in these two systems. Unless I am missing something, this comparison is not (but should be) plotted in Figure S5.

It was necessary to demonstrate a linear response between sulfate mass and [SO<sub>2</sub>,0] to illustrate that the sulfate particles were efficiently transmitted through the ACSM inlet aerodynamic lens (P5, L6-7). If they were not (e.g. too small or too large vs. the lens transmission window), we anticipate that the response would have been nonlinear.

We have revised Figure S4 (below; now Figure S6 in revised manuscript) to include the sulfate mass measured following SO<sub>2</sub> oxidation in the alkyl nitrite photolysis experiments compared with OFR254 experiments. The corresponding OH exposure for the alkyl nitrite systems was obtained by extrapolating the OFR254 calibration data to lower OH exposure.

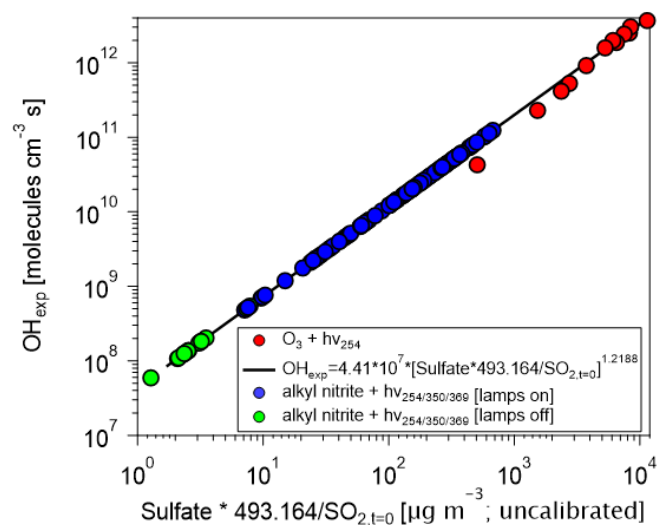


Figure S6. Calibrated OH<sub>exp</sub> obtained following reaction of 493 ppb SO<sub>2</sub> with OH generated via O<sub>3</sub>+ hv<sub>254</sub>→O(1D)+O<sub>2</sub> followed by O(1D)+H<sub>2</sub>O→2OH in the absence of NO<sub>x</sub> (red symbols). The calibration equation was applied to measurements of sulfate formed during alkyl nitrite photolysis experiments (blue symbols) where SO<sub>2</sub> was added at the

R2.4) Page 6, L18-19: How were the reductions in quantum yields for R6 and R5 determined? This seems like a critical assumption in the modeling and it is not explained in much detail. What is the sensitivity of the model predictions to these quantum yields?

We modified the text between L17-19 to clarify our rationales of this assumption. We also decide to change the upper limit quantum yield for Reaction R5 at 254 nm from 0.40 to 0.50 to reflect the value obtained by Raff and Finlayson-Pitts above 350 nm wavelength. The text now reads:

“At 254 nm, Calvert and Pitts (1966) estimated the quantum yield of Reaction R6 to be 0.86 under vacuum. **Assuming that all 254 nm photons initiate photolysis, the corresponding quantum yield of Reaction R5 is 0.14. Due to collisional deactivation at 1 atm that prevents  $i\text{-C}_3\text{H}_7\text{O}\cdot$  decomposition, the quantum yield of Reaction R5 at  $\lambda = 254$  nm and 1 atm is expected to be higher than 0.14. Because quantum yield measurements were unavailable at these conditions, we applied an upper limit quantum yield of 0.50 as applicable at  $\lambda > 350$  nm and 1 atm (Raff and Finlayson-Pitts, 2010). We calculated a corresponding nominal quantum yield of 0.32 by averaging the lower and upper limit values of 0.14 and 0.50, resulting in a quantum yield of 0.68 for Reaction R6.”**

Regarding the sensitivity of the model predictions to the quantum yield of Reaction R6, we modified text to Page 7, L29 to read:

**“Higher  $\text{NO}_2$  concentrations were modeled at  $\lambda = 254$  nm than at  $\lambda = 369$  nm because more  $i\text{PrONO}$  was photolyzed and the  $\text{NO}_2$  yield was only weakly dependent on the fate of  $i\text{-C}_3\text{H}_7\text{O}\cdot$ . For example,  $\text{NO}$  is converted to  $\text{NO}_2$  either via reaction with  $\text{HO}_2$  obtained via Reaction R5 or  $\text{CH}_3\text{O}_2\cdot$  and  $\text{CH}_3\text{C}(\text{O})\text{O}_2\cdot$  obtained via Reaction R6. However, the effect of photolysis wavelength on  $\text{NO}$  and  $\text{OH}_{\text{exp}}$  was different. Specifically, the highest  $\text{NO}$  concentration and  $\text{OH}_{\text{exp}}$  was achieved via OFR369- $i(i\text{PrONO})$ .  $\text{OH}_{\text{exp}}$  achieved via OFR369- $i(i\text{PrONO})$  was slightly higher than  $\text{OH}_{\text{exp}}$  attained using OFR350- $i(i\text{PrONO})$ , likely because photolysis of both  $i\text{PrONO}$  and  $\text{NO}_2$ , whose reaction with  $\text{OH}$  suppresses  $\text{OH}_{\text{exp}}$ , is more efficient at  $\lambda = 369$  nm than at  $\lambda = 350$  nm (Figure S1 and Table 1). Further, the  $\text{NO}$  and  $\text{OH}$  yields achieved via OFR254- $i(i\text{PrONO})$  were suppressed due to significant (>68%) decomposition of  $i\text{-C}_3\text{H}_7\text{O}$  (Calvert and Pitts, 1966). The products of  $i\text{-C}_3\text{H}_7\text{O}$  decomposition, i.e.,  $\text{CH}_3\text{CHO}$  and  $\text{CH}_3\cdot$ , both have adverse effects with regard to our experimental goals:  $\text{CH}_3\text{CHO}$  is reactive toward  $\text{OH}$  and can thus suppress  $\text{OH}$ ; the  $\text{RO}_2\cdot$  formed through this reaction,  $\text{CH}_3\text{C}(\text{O})\text{O}_2\cdot$ , consumes  $\text{NO}$  and generates  $\text{NO}_2$  but does not generate  $\text{OH}$ ;  $\text{CH}_3\cdot$  rapidly converts to  $\text{CH}_3\text{O}_2\cdot$ , which also consumes  $\text{NO}$  and generates  $\text{NO}_2$  but does not directly produce  $\text{OH}$ . The dependence of  $\text{OH}$ ,  $\text{NO}$  and  $\text{NO}_2$  on the quantum yields of Reactions R5 and R6 was confirmed by sensitivity analysis of uncertainty propagation inputs and outputs as described in Section 2.4.  $\text{OH}_{\text{exp}}$  and  $\text{NO}$  were strongly anticorrelated with the quantum yield of Reaction R6, whereas the correlation between  $\text{NO}_2$  and the quantum yield of Reaction R6 was negligible.”**

R2.5): The presentation of the equations in Page 10 needs to be improved. First, there seems to be a formatting issue – the first equation appears as equations 3-6 and the second as equations 7-9. Each equation should have one number. Second, I don’t understand where these equations came from. Where are the data these equations are fit to (it should at least be shown in the SI)? What is the quality of the fit? How was the functional form determined?

The equation formatting issue appears to be related to our attempt to implement multi-line equations using the Copernicus LaTeX template. We will follow up with the copy editing staff to resolve this issue.

To address the other questions from the reviewer, we modified text to Page 10, L11 to read:

“Fit coefficients were obtained by fitting Equations 3 and 6 to  $\text{OH}_{\text{exp}}$  model results over the following range of OFR parameters: ( $[\text{iPrONO}/\text{iPrONO-d}_7]$ ; 0.2-20 ppm),  $I_{369}$  ( $1 \times 10^{15}$  -  $2 \times 10^{16}$  photons  $\text{cm}^{-2} \text{s}^{-1}$ ),  $\text{OHR}_{\text{ext}}$  ( $1$ - $200 \text{s}^{-1}$ ), and residence time,  $\tau$ , between 30 and 200 sec. **We explored 11 logarithmically evenly distributed values in these ranges for each parameter, and thus performed simulations for 14641 model cases in total. To determine the functional form of Eqs. (3) and (6), we used the sum of the logarithms of first-, second-, and third-order terms of the four parameters and iteratively removed the terms with very small fit coefficients until further removal of remaining terms significantly worsened the fit quality.**”

We also modified text on Page 10, L20 to read:

“Thus, we derived  $\text{NO}_2$  estimation equations for OFR369-i(iPrONO) (Eq. 10) and OFR369-i(iPrONO-d<sub>7</sub>) (Eq. 11) as a function of  $[\text{RONO}]$ ,  $I_{369}$ , and  $\tau$ , **to all of which  $\text{NO}_2$  is roughly proportional**, over the same phase space of model results used to fit Eqs. 3 and 6:”

The output data points of the model runs for fitting estimation equations (and the corresponding quantities estimated by the fitted equations) had already been shown in Fig. S7 of the AMTD version. The mean absolute values of the relative deviations of the equation estimates from the model outputs had already been reported to be 29% and 19% in Page 10, L14 and 26 for  $\text{OH}_{\text{exp}}$  and  $\text{NO}_2$ , respectively.

R2.6) Section 3.5: The comparison between the OFR and ambient CIMS spectra are presented only as in-line text. This comparison would be more effective if done graphically.

To Figure 5 (Figure 6 in the revised manuscript) we added panels (e) and (f) containing ambient  $\text{NO}_3$ -CIMS spectra obtained from high- $\text{NO}_x$  photochemical conditions in Centreville, Alabama, USA (Massoli et al., 2018) and in Hyytiala, Finland (Yan et al., 2016) We implemented an additional suggestion by this reviewer to add a separate panel (d) showing the -OD containing sticks (see R2.24).



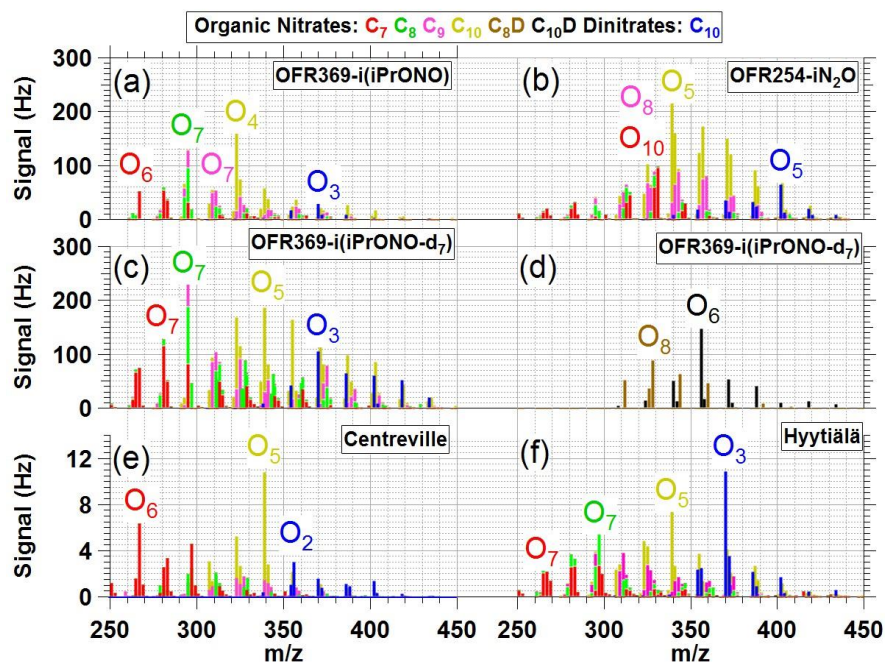


**Figure 6.**  $\text{NO}_3^-$ -CIMS spectra of nitrogen-containing  $\alpha$ -pinene photooxidation products with  $\text{C}_7\text{--}9\text{H}_9,11,13,15\text{NO}_5\text{--}10$  (“ $\text{C}_7$ ”,  $\text{C}_8$ ,  $\text{C}_9$ ”),  $\text{C}_{10}\text{H}_{15,17}\text{NO}_4\text{--}14$  (“ $\text{C}_{10}$ ”),  $\text{C}_8\text{H}_{8,10}\text{DNO}_8\text{--}14$  (“ $\text{C}_8\text{D}$ ”),  $\text{C}_{10}\text{H}_{14,16}\text{DNO}_7\text{--}14$  (“ $\text{C}_{10}\text{D}$ ”) or  $\text{C}_{10}\text{H}_{16,18}\text{N}_2\text{O}_6\text{--}13$  (“ $\text{C}_{10}$  dinitrate”) formulas generated via (a) OFR369-i(iPrONO) (b) OFR254-i $\text{N}_2\text{O}$  ( $\text{H}_2\text{O} = 1\%$ ,  $\text{N}_2\text{O} = 3.2\%$ ). (c,d) OFR369-i(iPrONO-d7) and observed in ambient measurements at (e) Centreville, Alabama, United States (Massoli et al., 2018) (f) Hyttiala, Finland (Yan et al., 2016). “Ox” labels indicate number of oxygen atoms in corresponding signals (excluding 3 oxygen atoms per nitrate

We modified the text as follows:

“The ability of OFR369-i(iPrONO) and OFR369-i(iPrONO-d7) to mimic polluted atmospheric conditions can be evaluated by comparing signals observed in Figure 6 with published  $\text{NO}_3^-$ -CIMS spectra obtained in Centreville, AL, USA (Massoli et al., 2018) and in Hyttiala, Finland (Yan et al., 2016). Both measurement locations are influenced by local biogenic emissions mixed with occasional anthropogenic outflow. **Figures 6e and 6f were obtained on 25 June 2013 (7:30–11:00 Centreville time) and 11 April 2012 (10:00–13:00 Hyttiala time) respectively. The mean  $\text{NO}$  mixing ratios during these periods were  $0.53 \pm 0.17$  (Centreville) and  $0.27 \pm 0.09$  ppb (Hyttiala).** In Centreville, the largest  $\text{C}_{10}$  nitrate and dinitrate species were  $\text{C}_{10}\text{H}_{15}\text{NO}_8$  and  $\text{C}_{10}\text{H}_{16}\text{N}_2\text{O}_8$ ; in Hyttiala,  $\text{C}_{10}\text{H}_{15}\text{NO}_8$  and  $\text{C}_{10}\text{H}_{16}\text{N}_2\text{O}_9$  were the largest  $\text{C}_{10}$  nitrate/dinitrate signals. Elevated  $\text{C}_{10}$  dinitrate levels during the daytime in Hyttiala (Figure 6f) suggests their formation from monoterpenes via two OH reactions followed by two  $\text{RO}_2 + \text{NO}$  termination reactions, as proposed earlier. Overall, Figure 6 shows that many of the  $\text{C}_7$ – $\text{C}_{10}$  nitrogen-containing compounds observed in Centreville and Hyttiala were generated via OFR369-i(iPrONO), OFR369-i(iPrONO-d7) and OFR254-i $\text{N}_2\text{O}$ . Due to the local nature of the ambient terpene emissions at the Centreville and Hyttiala sites, the associated photochemical

age was presumably <1 day. Thus, while the ambient NO<sub>3</sub><sup>-</sup>-CIMS spectra at those sites were more complex and contained contributions from precursors other than α-pinene, the oxidation state of the ambient terpene-derived organic nitrates was more closely simulated via OFR369-i(iPrONO) or OFR369-i(iPrONO-d<sub>7</sub>), where the largest C<sub>10</sub> nitrates and dinitrates were C<sub>10</sub>H<sub>15</sub>NO<sub>7</sub> and C<sub>10</sub>H<sub>16</sub>N<sub>2</sub>O<sub>9</sub> (OFR369-i(iPrONO); Figure 5a), and C<sub>10</sub>H<sub>15</sub>NO<sub>8</sub>, C<sub>10</sub>H<sub>15</sub>NO<sub>9</sub> and C<sub>10</sub>H<sub>16</sub>N<sub>2</sub>O<sub>9</sub> (OFR369-i(iPrONOd<sub>7</sub>); Figure 5c). By comparison, C<sub>10</sub>H<sub>15</sub>NO<sub>8</sub> and C<sub>10</sub>H<sub>16</sub>N<sub>2</sub>O<sub>11</sub> were the largest nitrate and dinitrate species generated via OFR254-iN<sub>2</sub>O (Figure 5b).”

R2.7) Relevance of this study for “Mimicking polluted atmospheric conditions”: the manuscript addresses a key limitation of the N<sub>2</sub>O-OFR, in which, achieving < 1 equivalent day of NO<sub>x</sub> dependent SOA formation is challenging. While the use of ANs as OH (or OD) precursors is shown to be promising for achieving such low oxidative exposures in this study, this potentially makes OH suppression a major concern for in-situ deployment of the AN-OFR (Peng et al. 2015). The chemical composition of α-pinene SOA formed in the AN-OFR (this study) bears resemblance to SOA previously observed in terpene-rich conditions in Centerville, Alabama and Hyytiälä, Finland (Yan et al., 2016; Massoli et al., 2018), suggesting that OH suppression may not be an issue. However, the manuscript lacks description of how much α-pinene was injected into the OFR, whether OH suppression was a competing influence, and if yes, whether or not it was accounted for.

We modified the text as follows:

P11, L3: “To evaluate the efficacy of OFR369-i(iPrONO), OFR369-i(iPrONO-d<sub>7</sub>), and OFR254-iN<sub>2</sub>O [...] the reactor was operated with a residence time of approximately 80 sec to accommodate the undiluted NO<sub>3</sub><sup>-</sup>-CIMS inlet flow requirement (10.5 L min<sup>-1</sup>). OFR369-i(iPrONO) and OFR369-i(iPrONO-d<sub>7</sub>) were operated using  $I_{369} = 6.5 \times 10^{15}$  photons cm<sup>-2</sup> s<sup>-1</sup>, >7 ppm nitrite, **and 500 ppb α-pinene**. OFR254-iN<sub>2</sub>O was operated using  $I_{254} = 3.2 \times 10^{15}$  photons cm<sup>-2</sup> s<sup>-1</sup>, 5 ppm O<sub>3</sub> + 1% H<sub>2</sub>O + 3.2% N<sub>2</sub>O, **and 16 ppb α-pinene**. Corresponding **calculated** OH exposures were  $2.9 \times 10^{10}$ ,  $5.9 \times 10^{10}$  and  $5.0 \times 10^{11}$  molecules cm<sup>-3</sup> s, respectively, **in the absence of OH consumption due to α-pinene. These calculated steady-state OH<sub>exp</sub> values decreased to  $8.5 \times 10^8$ ,  $6.8 \times 10^8$  and  $4.6 \times 10^{11}$  molecules cm<sup>-3</sup> s after accounting for OH consumption. This suggests that most of the OH that was produced in these OFR369-i(iPrONO/iPrONO-d<sub>7</sub>) experiments was consumed by α-pinene and its early-generation photooxidation products. We note that OH suppression relative to 254 nm photons, O<sub>3</sub>, and O is not a concern in OFR369-i(iPrONO), unlike OFR254-iN<sub>2</sub>O (Peng et al., 2016).**”

R2.8) Abstract line 3: extra “t” before λ.

Deleted (see also reply to R1.3).

R2.9) Equation 1: I assume that density is for the liquid, but please specify.

We modified the text as follows:



P3, L5-6: “where [...]  $\rho$  ( $\text{g cm}^{-3}$ ) and MW ( $\text{g mol}^{-1}$ ) are the organic nitrite **liquid** density and molecular weight...”

R2.10) P1 L17: space needed before (Mao et al., 2009...). This error repeats several times in citations throughout the manuscript.

We fixed this error in the revised manuscript.

R2.11) P2 L13: in the presence of humidified air (if I am understanding the reactions correctly).

No - water vapor is not required for  $\text{HO}_x + \text{NO}_x$  generation via alkyl nitrite photolysis.

R2.12) Page 3, L14: the light manufacturer LCD Lighting is listed in this line but not the previous lines.

Yes, LCD Lighting is the light manufacturer. The part numbers listed in previous lines (F436T5/BL/4P-350, F436T5/BLC/4P-369) were formatted per the preference of LCD Lighting, Inc., where they manufactured the lamps as OEM equipment and then renamed the end products with part # and reference to Aerodyne Research.

R2.13) P3 L18-23: Is it possible to include some numbers describing this interference (maybe in the SI)? How was the conclusion of “no avail” drawn? Did the 2B monitor read increasing [NO<sub>x</sub>] with increasing [iPrONO] injection into dark OFR? Since this AN photolysis is a unique aspect of this manuscript, I think instrumental caveats should be better described.

Yes, exactly - the 2B monitor read increasing [NO<sub>x</sub>] with increasing [iPrONO] injection into dark OFR (both NO and NO<sub>2</sub> channels).

We modified the text as follows:

P3, L18-23: “NO and NO<sub>2</sub> mixing ratios were measured using a NO<sub>x</sub> analyzer (Model 405 nm, 2B Technologies), which quantified [NO<sub>2</sub>] (ppb) from the measured absorbance at  $\lambda = 405$  nm, and [NO] (ppb) by reaction with O<sub>3</sub> to convert to NO<sub>2</sub>. Alkyl nitrites introduced to the reactor with the lamps turned off consistently generated signals in the both NO and NO<sub>2</sub> measurement channels of the NO<sub>x</sub> analyzer, possibly due to impurities **and/or species generated via iPrONO + O<sub>3</sub> reactios inside the analyzer. For example, background NO and NO<sub>2</sub> mixing ratios increased from 0 to 1526 ppb and 0 to 1389 ppb as a function of injected [iPrONO] = 0 to 18.7 ppm with the lamps off (Figure S2).** We attempted to correct [NO] and [NO<sub>2</sub>] for this apparent alkyl nitrite interference by subtracting background signals measured in the presence of alkyl nitrite with lamps off, to no avail, **because background signals (alkyl nitrite present with lamps off) were large compared to signals obtained with alkyl nitrite present with lamps on.** Instead, we constrained [NO] and [NO<sub>2</sub>] using the photochemical model discussed in Section 2.4.”

We added a figure to the supplement (below):

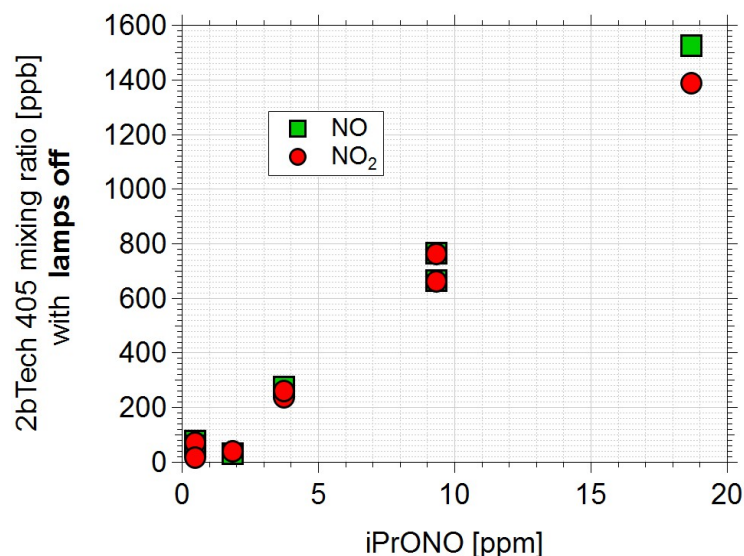


Figure S2. “NO” and “NO<sub>2</sub>” mixing ratios measured at the exit of the reactor as a

R2.14): Somewhere in the methods section, the authors should mention what was the flow through the OFR in the calibration experiments. The flow rate through OFR for CIMS experiments is mentioned later, but the flow rate in non-CIMS experiments is not mentioned anywhere.

We modified the text as follows:

P3, L11: “Alkyl nitrites were photolyzed inside a Potential Aerosol Mass (PAM) oxidation flow reactor [...] operated in continuous flow mode (Lambe et al., 2017) with **5.1±0.3 L/min flow through the reactor unless stated otherwise.**”

R2.15) P8 L5: this sentence is confusing, because it suggests that measured values of NO<sub>x</sub> are shown in Figure 3, while in fact they are not. Should be reworded accordingly.

The original sentence read: “Figure 3 shows measured and modeled OH<sub>exp</sub> and NO<sub>x</sub> Concentrations”. We reworded the sentence to state: “Figure 3 shows measured OH<sub>exp</sub> and **modeled** NO<sub>x</sub> concentrations.”

R2.16) P8 L30 (and Figure 4): the explanation of higher NO<sub>x</sub> offsetting OH production efficiency seems straightforward enough that it should be reproduced by KinSim. However, it seems the model was not run (or not plotted in Figure 4) for this OFR369-i(1,3-Pr(ONO)<sub>2</sub>) scenario. Can this be explained?

Constraints on the OH rate constant and absorption cross section of 1,3-Pr(ONO)<sub>2</sub> are required to model OFR369-i(1,3-Pr(ONO)<sub>2</sub>). In this case, literature values were not available and we did

not feel we could adequately constrain the rate constant and cross section from first principles or structure-activity relationships.

R2.17): Again, the caption for Figure 4 is confusing because “measured and modeled values ... of (iPrONO-d7) and (1,3-Pr(ONO)<sub>2</sub>)” suggests that the modeled values for BOTH these precursors are plotted, while in fact the model was apparently not run for the latter precursor (this goes back to my previous comment).

We modified the Figure 4 caption as follows:

“OH<sub>exp</sub> values measured as a function of I<sub>369</sub> following photolysis of perdeuterated isopropyl nitrite (iPrONO-d<sub>7</sub>) and 1,3-propyl dinitrite (1,3-Pr(ONO)<sub>2</sub>). Modeled OH<sub>exp</sub> values obtained from OFR369-i(iPrONO-d<sub>7</sub>) and OFR369-i(iPrONO) (Fig. 2d) are shown for reference....”

R2.18): Sections 3.3.1 and 3.3.2: are these sub-sections relevant to their parent section 3.3? The parent section title only mentions (iPrONO-d<sub>7</sub>) and (1,3-Pr(ONO)<sub>2</sub>). In fact, are these subsections even important enough to be placed in this part of the manuscript? There was no prior discussion of why MeONO and HFiPrONO are important OH precursors. These sub-sections abruptly build up the importance of these two precursors, and then rapidly declare that they are not suitable precursors in the OFR. The narrative flows smoother going directly from experimentally measuring OH<sub>exp</sub> to setting up estimation equations i.e., from P8 L33 directly to P9 L27. I suggest moving 3.3.1 and 3.3.2 to the end of the manuscript or to the SI.

We moved Section 3.3.1 (MeONO), Section 3.3.2 (now HONO, per reply to R2.1), and Section 3.3.3 (HFiPrONO) to a new Section 3.5 titled: “Anticipated performance of alternative high-NO<sub>x</sub> HO<sub>x</sub> precursors in OFRs”

R2.19): Sections 3.2 and 3.3 are really hitting the same hammer (how much OH<sub>exp</sub> is generated from precursor X) on different nails (X = iPrONO, deuterated iPrONO, etc.). I don't see why they need to be separate sections.

We prefer to maintain separate sections for discussion of iPrONO, which presumably will be more widely used, and synthesized alkyl nitrites, which we assume will be used by advanced users. We instead combined the current Sections 3.1 and 3.2 into a single section 3.1 titled “OH<sub>exp</sub> and NO<sub>x</sub> generated from iPrONO photolysis” with subsections 3.1.1 “Effect of photolysis wavelength” and 3.1.2 “Effect of alkyl nitrite concentration”.

R2.20): Figure S7b is missing a 1:1 line.

We added the 1:1 line.

R2.21): P10 L18: NO<sub>2</sub> needs a subscript.

We added the subscript.

R2.22): P11 L5: OFR operation details (flow rate, etc.) should be described in the Section 2.3. Also, amount of  $\alpha$ -pinene injected into OFR should be mentioned to give a sense of the OHR.

We moved some content from P11, L5 to Section 2.3, which now reads as follows:

“In a separate set of experiments, mass spectra of gas-phase  $\alpha$ -pinene photooxidation products were obtained with an Aerodyne high-resolution time-of-flight chemical ionization mass spectrometer (Bertram et al., 2011) using nitrate as the reagent ion ( $\text{NO}_3^-$ -HRTof-CIMS, hereafter abbreviated as  $\text{NO}_3^-$ -CIMS) (Eisele and Tanner, 1993; Ehn et al., 2012). [...] The  $\text{NO}_3^-$ -CIMS sampled the reactor output at  $10.5 \text{ L min}^{-1}$ .  $\alpha$ -Pinene oxidation products were detected as adduct ions of  $\text{NO}_3^-$ . **In these experiments, the reactor was operated with a residence time of approximately 80 sec to accommodate the undiluted  $\text{NO}_3^-$ -CIMS inlet flow requirement. OFR369-i(iPrONO) and OFR369-i(iPrONO-d<sub>7</sub>) were operated using  $I_{369} = 6.5 \times 10^{15} \text{ photons cm}^{-2} \text{ s}^{-1}$  and  $>7 \text{ ppm alkyl nitrite}$ . In these experiments,  $\alpha$ -pinene was evaporated into the carrier gas by flowing 1 sccm  $\text{N}_2$  through a bubbler containing liquid  $\alpha$ -pinene. Assuming the  $\text{N}_2$  was saturated with  $\alpha$ -pinene vapor, we estimate  $\sim 500 \text{ ppb } \alpha$ -pinene was introduced to the OFR based on its vapor pressure at room temperature and known dilution ratio into the main carrier gas. In a separate experiment, OFR254-i $\text{N}_2\text{O}$  was operated using  $I_{254} = 3.2 \times 10^{15} \text{ photons cm}^{-2} \text{ s}^{-1} + 5 \text{ ppm } \text{O}_3 + 1\% \text{ H}_2\text{O} + 3.2\% \text{ N}_2\text{O}$ . Here,  $\alpha$ -pinene was introduced by flowing 1 sccm  $\text{N}_2$  of a gas mixture containing 150 ppm  $\alpha$ -pinene in nitrogen (unavailable for the iPrONO photolysis experiments) into the main carrier gas.”.**

R2.23): P11 L11: compound nomenclature is missing some subscripts.

We added missing subscripts to “[ $(\text{NO}_3)\text{C}_7\text{H}_9\text{NO}_8^-$ ]” and “[ $(\text{NO}_3)\text{C}_7\text{H}_{11}\text{NO}_8^-$ ]”

R2.24): P11 L20: this is a cool finding but does not readily jump out in Figure 5. I suggest adding a fourth panel showing a difference between the 5b and 5c (or 5a) spectra and zooming in the m/z scale to show the just a few –OD containing sticks (e.g., from m/z 310 to 360).

We implemented the reviewer’s suggestion (please see R2.6).

R2.25) Figure 5: There is enough empty space in each subfigure to include the dinitrite:nitrite ratio value. I suggest adding this in to quantify the “highest ratios observed in 5b” statement on P11 L24.

The revised figure has 6 panels and consequently less empty space to include the dinitrate:nitrate ratio. However, we modified the text to include the dinitrate fractions:

P11, L24: “Second,  $\text{C}_{10}$  dinitrates were present in all three spectra, with the highest dinitrate:nitrate **fractions** observed in Figures 5b (**0.090**) and 5c (**0.081**) and the lowest dinitrate:nitrate **fraction** observed in Figure 5a (**0.056**).

R2.26) Figure S7: units of  $OH_{exp}$  are incorrect on both X- and Y-axes (s, not s-1).

We changed the units of  $OH_{exp}$  from  $\text{molec cm}^{-3} \text{s}^{-1}$  to  $\text{molec cm}^{-3} \text{s}$ .